FYN tyrosine kinase, a downstream target of receptor tyrosine kinases, modulates anti-glioma immune responses

Andrea Comba[1,2], Patrick J Dunn[1,2], Anna E Argento[1,2], Padma Kadiyala[1,2], Maria Ventosa[1,2], Priti Patel[1,2], Daniel B Zamler[1,2], Felipe J Nunez[1,2], Lili Zhao[3], Maria G Castro[1,2], Pedro R. Lowenstein[1,2]

[1]Department of Neurosurgery, University of Michigan Medical School, Ann Arbor, MI 48109

[2]Department of Cell and Developmental Biology, University of Michigan Medical School, Ann Arbor, MI 48109

[3]Department of Biostatistics, University of Michigan Medical School, Ann Arbor, MI 48109

Running title: FYN modulates suppressive glioma immune responses

Corresponding Author: Pedro R Lowenstein. Department of Neurosurgery University of Michigan School of Medicine, 1150 West Medical Center Drive, MSRB II, Room 4570, Ann Arbor, MI 48109-5689. Phone (office) 734-764-0851. Email: pedrol@umich.edu

Conflicts of Interest

All authors of this paper declare no potential conflicts of interest.

Authorship

Conception and design: A. Comba and P.R. Lowenstein.

Development of methodology: A. Comba, P.J. Dunn, A.E. Argento, P. Kadiyala, P.R. Lowenstein.

Acquisition of data, analysis and Interpretation A. Comba, P.J. Dunn, A.E. Argento, P. Kadiyala, M. Ventosa, P. Patel, D.B. Zamler, F.J. Nunez, L. Zhao, M.G. Castro, P.R. Lowenstein.

Manuscript writing: A. Comba, P.J. Dunn, M.G. Castro, P.R. Lowenstein.

Review, and/or revision of the manuscript: A. Comba, P.J. Dunn, A.E. Argento, P. Kadiyala, M. Ventosa, P. Patel, D.B. Zamler, F.J. Nunez, L. Zhao, M.G. Castro, P.R. Lowenstein.

Administrative, technical, or material support (i.e., reporting or organizing data, constructing databases): A. Comba, P.J. Dunn, P.R. Lowenstein.

Study supervision: M.G. Castro and P.R. Lowenstein.

Manuscript word count: 5986 total manuscript word count, including words in abstract, text, references, and figure legends

ABSTRACT

Background: High grade gliomas are very aggressive and immunosuppressive brain tumors. Molecular mechanisms that regulate the inhibitory immune tumor microenvironment (TME) and glioma progression remain poorly understood. FYN tyrosine kinase is a downstream target of the oncogenic receptor tyrosine kinases pathway and is overexpressed in human gliomas. FYN's role *in vivo* in glioma growth remains unknown. We aimed to study whether FYN regulates GBM growth and invasion.

Methods: We evaluated the role of FYN using genetically engineered mouse models (GEMM) of glioma. We also generated FYN knockdown stem cells to induce gliomas in immune-competent and immune-deficient mice (NSG and CD8-/-). We analyzed molecular mechanism by RNA-Seq and bioinformatics analysis. Flow cytometry was used to characterize immune cellular infiltrates in the FYN knockdown glioma TME.

Results: We show that FYN knockdown in diverse immune-competent GEMM of glioma reduced tumor progression and significantly increased survival. GSEA analysis of DE genes in WT vs. FYN knockdown gliomas showed enrichments of gene ontologies related to immune reactivity. However, in NSG and CD8-/- immune-deficient mice, FYN knockdown glioma failed to show difference in survival. These data suggest that the expression of FYN in glioma cells reduces anti-glioma immune activation. Examination of glioma immune infiltrates by flow-cytometry displayed reduction in the amount of immune inhibitory myeloid derived cells (MDSCs) in the FNY glioma TME.

Conclusions: Gliomas employ FYN mediated mechanisms to suppress the immune system and promote tumor progression. Selective inhibition of FYN within glioma cells could improve the efficacy of anti-glioma immunotherapies.

Keywords

Fyn Tyrosine kinase, Glioma, Anti-tumor immune responses, Myeloid-derived suppressor cells

Key points

Inhibition of FYN tyrosine kinase in genetically engineered mouse glioma models delays tumor progression. The oncogenic effects of FYN in vivo are mediated by downregulation of anti-glioma immunity.

Importance of the Study

FYN is an effector of RTK signaling in glioma. However, its role *in vivo* remains unknown. Our study demonstrates that FYN tyrosine kinase is a novel regulator of the anti-glioma immune response. We show that FYN inactivation suppresses glioma growth, increases survival, and enhances anti-tumor immune reactivity. Our findings suggest that suppressing the expression of FYN in glioma cells could provide a novel therapeutic target.

INTRODUCTION

Glioblastoma multiforme, or high grade glioma (HGG) is the most frequent and aggressive primary tumor of the central nervous system. It is characterized by extensive infiltrative growth and resistance to therapy[1]. Mutated/activated driver genes such as the receptor tyrosine kinases (RTK: EGFR, PDGFR, HGF/MET), tumor suppressor genes (TP53, PTEN/NF1) and downstream RAS/PI3K/MEK pathways contribute to the malignity of glioma [2]. FYN, a non-RTK member of the SRC tyrosine kinase family (SFK), is a downstream proto-oncogene target of the RTK pathway, [3-6]. However, the specific mechanisms by which FYN stimulates glioma growth and invasion remains unknown. FYN is rarely mutated [7] in human HGG, but is significantly overexpressed.

Several *in-vitro* studies showed that FYN knockdown is associated with decreased cell migration and proliferation of glioma cells [3,8,9]. Nevertheless, *in vivo* human glioma xenograft models of FYN Knockdown in immune-suppressed animals failed to show any difference in survival [8]. Therefore, an immune-competent mouse model that enables the generation of FYN knockdown gliomas amenable for understanding the mechanism of anti-glioma immune response is essential.

In this study we demonstrate that FYN, a downstream target of receptor tyrosine kinases signaling, inhibits the anti-glioma immune response. We demonstrated that FYN tyrosine kinase promotes glioma growth utilizing both immune-competent and immune-deficient mouse glioma models. We observed that implantation of FYN knockdown tumors into immune-competent mice significantly prolonged their survival compared to wildtype FYN tumor bearing mice. However, implantation of FYN knockdown tumors into immune-deficient mice did not have an effect on their survival. Molecular analysis revealed a significant upregulation of immune gene ontologies in shFYN tumors. Our data suggest that FYN expression in glioma cells suppresses the immune responses by mediating the expansion of MDSCs in glioma tumor microenvironment (TME). Gliomas have been demonstrated to employ a variety of immunosuppressive mechanism which promotes tumor progression, thus reducing the effectiveness of immunotherapies [10,11].

Our data uncover a new paradigm of how FYN tyrosine kinase expressed by the tumor cells regulates the anti-glioma immune responses. We propose that tumor cell specific inhibition of FYN tyrosine kinase increases the sensitivity of gliomas to immune attack, which could be a target for future treatments of glioma patients.

MATERIALS AND METHODS

Glioma cells

Mouse neurospheres cells were derived from genetically engineered mouse models (GEMM) of gliomas. These cells were generated in our lab using the Sleeping Beauty (SB) transposon system [12,13]. The human glioma derived stem cells called MGG8 was obtained from Samuel Rabkin, Harvard University. All cells were cultured as described in Supplementary data.

In vitro cell treatments

Cells were treated with Saracatinib (AZD0530) a SRC family pan inhibitor (Selleck Chemicals, Houston, TX) as detailed in Supplementary data [14].

In vitro cell viability assay

Cell viability was analyzed using the CellTiter-Glo® Luminescent Assay (Promega Corp. Madison, WI, US) as recommended by the manufacturer.

In vitro cell migration assay

Transwell migration set up was utilized to determine cell migration *in vitro*. Transwell® polycarbonate membrane inserts (Corning Inc.) of 6.5 mm diameter and 8 um pore size were used for all assays. Detailed methodology is described in Supplementary data.

Generation of stable cell lines with FYN knockdown

NP and NPA neurospheres were used to generate stable cell lines with FYN knockdown. The pLenti pLKO-non-target shRNA control vector (SHC002) and two different pLenti-mouse shRNA vectors for FYN were selected from Sigma Aldrich MISSION® shRNA Vectors. The FYN shRNA identification numbers are: TRCN0000023383 (shFYN #1) and TRCN0000361213 (shFYN #2).

Cells were infected with the lentivirus as described previously by us [15]. Immunoblotting was used to confirm FYN knockdown. FYN shFYN #2 cells were selected for *in vivo* experiments.

Intracranial implantable syngeneic mouse glioma model

Studies were conducted according to the guidelines approved by the Institutional Animal Care (IACUC) and Use Committee at the University of Michigan (approved protocol, PRO00007666 for C57BL/6 immune-competent mice and PRO00007669 for immune-suppressive mice). 3.0 x 10^4 neurospheres were implanted into the striatum of mouse brains to generate tumors. See supplementary data.

Genetically engineered mouse glioma model (GEMM) generation for FYN Knockdown

The animal model studies were conducted in C57BL/6 mice (Jackson Laboratory), according to IACUC approved protocol PRO00007617. A FYN knockdown glioma murine model and the appropriate controls were created by the Sleeping Beauty (SB) transposon system as described [12,13]. The genotypes of SB generated tumors were: (i) shp53 and NRAS **(NP)**, (ii) shp53, NRAS and shFYN **(NPF)**, (iii) shp53, NRAS and shATRX **(NPA)**, (iv) shp53, NRAS, shATRX and shFYN **(NPAF)**, (v) shp53, NRAS and PDGFβ **(NPD)**, (vi) shp53, NRAS, PDGFβ and shFYN **(NPDF)**. Design and cloning of shFYN vector is in Supplementary data.

Immunoblotting

Glioma cells (1.0 x 10^6 cells) were seeded in a 100 mm dish and grown at various time points as shown in supplementary data.

Immunohistochemistry of paraffin embedded brains (IHC-DAB)

Immunohistochemistry assay was performed on paraffin embedded tissue as described previously[16].

Immunofluorescence of paraffin embedded brains

Brains that were fixed in 4% paraformaldehyde were processed, embedded in paraffin and sectioned as described previously [16]. FYN antibody was conjugated with Alexa Fluor™ 488 Tyramide SuperBoost™ Kit - Goat Anti-Rabbit IgG (# B40922) following the manufacture instructions (Invitrogen- Thermo Fisher Scientific).

RNA isolation and RNA-Sequencing

SB NP vs. NPF tumors were studied by RNA-Seq analysis. RNA was isolated using the RNeasy Plus Mini Kit (© QIAGEN) following the manufacture instructions. RNA-sequencing was performed at the University of Michigan DNA Sequencing Core. Detailed analysis is described in Supplementary data.

Flow Cytometry

For flow cytometry analysis of immune cells within the TME, we generated tumors by intracranial implantation of 3.0 x 10^4 NPA-NT and NPA-shFYN cells in C57Bl6 mice. Protocol was performed as described before (REF Neha) and detailed in Supplementary data.

Statistical Analysis. All experiments were performed in at least three or more independent biological replicates, depending on the specific analysis. Data is presented as the mean ± SEM. All statistical tests used are indicated within the figure legends and in Supplementary data.

RESULTS

FYN was identified as a potential regulator of glioma progression

FYN tyrosine kinase is connected to the downstream signaling pathways of commonly mutated genes in gliomas, such as EGFR, PDGR, MET and RAS/AKT **(Fig 1A).** We analyzed RNA-Sequencing and Microarray human data from the Gliovis (http://gliovis.bioinfo.cnio.es) database. According to Rembrandt, TCGA, and Gravendeel databases, FYN mRNA expression levels were higher in different types of human gliomas when compared to normal brain tissue **(Supplementary Fig. S1A)**. Western blot (WB) analysis of mouse and human glioma stem cells revealed FYN protein levels to be higher in tumor cells that are malignant, as previously described.[17] **(Fig. 1B).** To further analyze the importance of FYN in glioma malignancy, we investigated differential expression (DE) of genes in phenotypically aggressive NPA-neurospheres (NRAS, shp53, shATRx, IDH-Wild-type) and also in less malignant NPAI-neurospheres (NRAS, shp53, shATRx, $IDH1^{R132H}$) [13]. The network of DE genes identified FYN to be one of the most highly connected nodes (Degree: 63; 4th node from top node), a hub in the network **(Fig. 1C-D).** To analyze the role of FYN in human glioma derived stem cells, we extended our network analysis to two human glioma stem cells of differential aggressiveness (MGG8-adherent vs MGG8-Spheres cells) [17]. This analysis also revealed FYN to be a hub in the network (Degree: 47; 7th node from top node) **(Fig. 1E-F)**. **Fig. (1D)** and **(1F)** display the network of FYN, a set of nodes directly connected to FYN. Detailed information of genes present in each of networks is shown in **Supplementary Table S1 A-B**. Functional network GO term analysis from both networks disclose Cell Proliferation, Cell migration, MAPK cascade, Cellular response to PDGF as significant GO Biological Processes involving FYN **(Supplementary Fig. 1B)**. The full list of GO terms is shown in **Supplementary, Tables S2A-B** and **S2C-D** respectively.

Saracatinib impairs cell viability and migration *in vitro*, but does not impact tumor progression and survival *in vivo*.

FYN tyrosine kinase acts as a potential regulator of glioma growth and malignancy. We determined whether inhibiting FYN activity has an effect on *in vitro* proliferation and migration of glioma cells. WB analysis of NP and NPA stem cells treated with SFK inhibitor, Saracatinib, inhibited SFK activation (Y416 activation site phosphorylation and Y530 inactive site). Levels of FYN protein were unchanged post Saracatinib treatment **(Supplementary Fig. S2A)**. Saracatinib significantly decreased cell viability and cell migration in NP and NPA stem cells in a dose-dependent manner (**Supplementary Fig. S2B-D**). *In vivo,* despite a clear reduction in the phosphorylation of the active site (Y416) we did not observe extension in survival after Saracatinib treatment (**Supplementary Fig. S2E-F**). These results indicate that SFK inhibition is not specific for FYN inhibition.

Loss of FYN reduces tumor malignancy and prolongs survival of mice harboring GEMM tumors.

The Sleeping Beauty Transposon System GBM model (GEMM) was used to understand the function of FYN [12]. We generated a FYN-deficient genetically engineered mouse glioma model (**Supplementary Fig. S3A and B**). We corroborated the efficacy of the shRNAs of FYN by WB analysis (**Supplementary Fig. S3C**). The shFYN-(b) was selected for the GEMM glioma generation. We generated tumors harboring wildtype or FYN knockdown in the presence of various genotype combinations (**Supplementary Fig. S3D**).

Downregulation of FYN increased median survival (MS) in comparison to wildtype FYN control groups (**Fig. 2A, B and C**) in all genotype models. NPF group displayed an increased MS of 131 days compared with 94 days in the NP control group (**Fig. 2A**). The experimental group with knockdown of FYN in the context of ATRX loss (NPAF) exhibited an increased survival (MS: 142 days) compared with the NPA control (MS: 80 days), (**Fig. 2B**). In the third experimental group, FYN knockdown plus PDGFβ ligand upregulation (NPDF), also displayed an increased MS of 108 days compared with the NPD control group (MS: 69 days) (**Fig. 2C**). We corroborated the

downregulation of FYN protein in all experimental groups as shown in **Fig. 2D, 2E** and **2F** respectively. Histopathology analysis of tumors showed no evidence of significant differences in glioma malignant pathological markers (**Fig. 2G, H, I and J**). We further evaluated cellular proliferation of the tumor. Quantification demonstrated a significant decrease in the ratio of P-H3-S10 cells per total cells in FYN knockdown groups (**Fig. 2K, I and M**). These data demonstrate that FYN downregulation increases animal survival by decreasing tumor development and proliferation.

RNA-Seq and bioinformatics analysis reveal enhanced immunogenicity in FYN knockdown glioma models

RNA-sequencing and bioinformatics analysis was used to uncover the mechanism by which FYN knockdown leads to the inhibition of tumor growth and progression. These studies were performed on NP vs NP-shFYN engineered gliomas. RNA-Seq analysis revealed a group of 567 differentially expressed genes (226 upregulated genes and 341 downregulated genes (**Fig. 3A**). Using network analysis (Cytoscape) we analyzed the functional interaction of the DE genes resulting from FYN knockdown (**Fig. 3B**). In the network analysis, the following pathways were overrepresented: Extracellular matrix organization, β1 integrin cell surface interactions, signaling by PDGF, ECM-receptor interaction, signaling by interleukins and IFNγ among others (**Fig. Supplementary 4A and Supplementary Table S3**). In addition, the analysis of the network interactions revealed several genes which represent the leading regulators of the network (**Fig. 3B**). These genes were part of different functional modules, formed by highly interacting group of genes in the network (**Fig. 4C**). We found that STAT1 module (M1), is represented as the central module of the network. This module regulates immune functions, JAK-STAT pathways, cell differentiation of Th1, Th2 and Th17, IFNγ signaling, T cell activation and NK cell mediated cytotoxicity. We also identified other modules such as the ITGA (M0), which regulates extracellular matrix organization, ECM receptor interactions, and integrin signaling; the GNA14 module (M2), which modulates the Wnt

signaling pathways and the cadherin signaling pathways; the CAMK2A module (M4), which is involved in cAMP signaling, EGFR and PDGF signaling, and RAF/MAP kinase cascade. **(Fig. 3C)**.

The Gene Ontologies (GO) identified by gene set enrichment analysis (GSEA) suggest that FYN knockdown mediates an activation of immune response in GEMM. The analysis showed 24 GO terms that were significantly upregulated in NPF group at FDR < 0.1 and nominal p-value < 0.05 (**Fig. 4A**). However, we did not identify downregulated GO terms in NPF at a FDR <0.1 and p-value <0.05. Detailed enrichment results are shown (**Supplementary Table S4A and S4B)**. Upregulated GO terms indicated that "Cell Chemotaxis" (FDR: 5.94E-04 and NES: 2.68) and "Immune response" (FDR: 0.016 and NES: 2.29) are some of the most significantly enriched GO biological functions elicited by FYN downregulation (**Fig. 4B**). The analysis also included significant immune related GO terms such as: "Leukocyte Chemotaxis", "Innate Immune Response", "Response to Interferon Gamma" and "Adaptive Immune Response (**Fig. 4B**)". These GO terms are involved in the mechanism by which FYN knockdown decreases glioma malignancy. Details of the selected GO terms are shown in **Supplementary Table S5A-F**. The heat map mRNA expression analysis on the immune related GOs, exhibited significant increased levels of genes, such as: STAT1 (q-value=0.04), CIITA (q-value=0.004), IRF1 (q-value=0.01), IRF8 (q-value=0.004) NLRC5 (q-value= 0.004) and TAP1 (q-value= 0.009), IFNG (q-value=0.004), CXCL9 (q-value=0.004), CCL1 (q-value= 0.004) and CCL5 (q-value= 0.04) (**Fig. 4C**).

The role of FYN in glioma growth, malignancy, and immune response interaction

To test the hypothesis that FYN depletion stimulates the anti-tumor immune system *in vivo,* we implanted FYN knockdown cells in immune-competent and immune-deficient mice. We identified that downregulation of FYN leads to a decrease in phosphorylation of the SFK active site P-Y416,

however dos not have an effect on the Src expression, confirming the specificity of the shFYN (**Supplementary Fig. S5A and B**).

The *in vivo* study showed that inactivation of FYN in glioma cells strongly suppress tumor growth and increase survival in immune-competent mice (C57BL/6) **(Fig. 5A-B)**, but the effects in immune-compromised (NSG) mice was negligible (**Fig. 5C-F**). FYN knockdown group displayed a MS of 34 days compared to the NP- NT control group (MS: 27 days) (**Fig 5A**). Also, NPA-shFYN had a significantly higher median survival (MS: 30 days) than the NPA-NT control group (MS: 20) (**Fig. 5B**). Moreover, *in vivo* bioluminescence analysis of the tumors at 13 dpi showed that NP-FYN knockdown tumors exhibited lower signal. Tumor size evaluation at necropsy showed a correlation with *in vivo* tumor bioluminescence analysis (**Supplementary Fig. 5C and D**). These results validate the role of FYN in immune-competent mice. However, tumor induction in NSG immune-deficient mice with NP-shFYN tumors did not exhibited a significant difference in survival when compared to the control NP-wtFYN tumors (MS: 24 vs 26 dpi) **(Fig. 5C).** In mice bearing NPA-shFYN tumors a minor, yet statistically significant increase in MS (22 vs 24 dpi) was observed (**Fig. 5D**). Moreover, implantation of NP-shFYN and NPA-shFYN tumors in CD8 Knockout mice showed no difference in survival compared to the controls tumor bearing mice **(Fig. 5E-F).** Collectively, these results demonstrate that FYN downregulation enhances anti-tumor immune response.

FYN downregulation in glioma reduces Myeloid derived suppressive cells (MDSC) within the tumor microenvironment

To determine whether downregulation of FYN in gliomas has an effect on the immune response, we examined the immune cellular infiltrates in the TME. First, we analyzed the role of T cells in the TME of shFYN tumors. No significant difference in the frequency of $CD4^+$ T cells ($CD45^+$, $CD3^+$, $CD4^+$) or $CD8^+$ T cells ($CD45^+$, $CD3^+$, $CD8^+$) were observed in NPA-NT versus NPA-shFYN tumors (**Fig. 6A, B, C and D**). In gliomas, increases in MDSCs are an important mechanism of

anti-tumor immune evasion [18]. Therefore, we evaluated the expansion of MDSCs mediated immunosuppression in glioma TME. MDSCs were identified as monocytic M-MDSC ($CD45^+$, $CD11b^+$, $Ly6C^{hi}$, $Ly6G^-$) or polimorphonuclear PMN-MDSC ($CD45^+$, $CD11b^+$, $Ly6C^{lo}$, $Ly6G^+$). Interestingly, we observed a 1.79-fold decrease of M-MDSC (**Fig. 6E and 6G**) and a 3.04-fold decrease of PMN-MDSC (Fig. **6F and 6G**) in the TME of NPA-shFYN gliomas compared to NPA-NT controls. This suggests that downregulation of FYN in glioma reduced MDSC suppressive activity in the TME. Furthermore, we analyzed the expansion and activation status of and macrophages. We did not observe a significant increase in the frequency of macrophages ($CD45^+$, $CD11c^-$, $F4/80^+$) (**Fig. 6H and I**). The expression MHCII on macrophages in the TME was increased by 1.4-fold in NPA-shFYN gliomas versus NPA-NT controls (**Fig. 6J and K**). Our data suggest that FYN knockdown triggers an anti-glioma immune response potentially through downregulation of inhibitory MDSCs.

DISCUSSION

In this study we demonstrate that glioma-cell specific genetic inhibition of FYN tyrosine kinase increases anti-glioma immune-responses, thus significantly delaying tumor progression.

FYN is an effector of the RTK (EGFR, MET, PDGFR) pathway in glioma and other cancers RTK are commonly mutated drivers in high grade gliomas; yet their detailed downstream signaling pathways remain incompletely understood [3,4,19-21].

Molecular analyses of high grade glioma from the Rembrandt, TCGA and Gravendeel databases[7], and data from Lu *et al* [3], indicate increased expression of FYN. These human data correlate with our results in mouse models of high-grade gliomas, in which increased levels of FYN expression correlate with higher glioma aggressiveness. Further, our molecular gene interaction network analysis highlights FYN as a central network hub, suggesting it might function as a potential regulator of glioma malignancy.

Previous studies have shown that FYN is expressed by both tumor cells and immune cells [22]. In T cells, FYN regulates effector functions and amplifies T-cell antigen receptor (TCR) signaling [4,19,21,23]. However, it has been difficult to establish the role of FYN within glioma in vivo. The function of FYN can be studied genetically (i.e. knockdown) or pharmacologically (i.e. Saracatinib, or Dasatinib inhibitors). Genetic inhibition is highly specific. Pharmacological inhibition, however, is non-specific. Saracatinib or Dasatinib will inhibit all SFK members and will inhibits SFK in all cell types i.e. FYN in the immune cells.

For instance, *in vitro* studies using SFK inhibitors show that FYN promotes cell proliferation and migration in gliomas [3,9,14,24]. *In vivo*, effects of Saracatinib treatment have been mixed, yet unable to determine any specific role of FYN in glioma growth [3,8]. Importantly, Dasatinib, did not extend survival of glioma patients in a Phase II clinical trial [25]. Our *in vitro* experiments confirm that Saracatinib decreases glioma cell migration and cell proliferation. *In vivo* however, there was no effect on animal survival.

As Saracatinib and Dasatinib are non-specific inhibitors of individual SFK member [26], the genetic inhibition of FYN remains the best option to study its functions in glioma biology. Indeed, genetic downregulation of FYN expression inhibited glioma cells migration and proliferation *in vitro* [3,8,9,27], yet failed to affect glioma progression *in vivo* immune suppressive mice [8].

To address this paradox, we developed a genetic approach to inhibit FYN expression in tumor cells using a GEMM model of glioma in immune competent animals. Our results suggest that shFYN delays tumor progression *in vivo* by inhibiting the anti-glioma immune response.

We demonstrated the role that FYN plays a central hub in the anti-glioma immune response and tumor progression by inducing tumors in immune-deficient animals. The effect of FYN in delaying tumor growth was abolished in NSG and CD8-/- immune deficient animals. These studies suggest that FYN plays a crucial role in conveying immune inhibitory messages from within the glioma cells to the immune cells, thereby engineering the local immune response to favor tumor growth. Herein, we uncovered a new cell-non-autonomous mechanism by which FYN knockdown within glioma cells modulates the anti-glioma immune responses.

Analysis of the molecular changes induced by shRNA-FYN strongly suggests that the downregulation of FYN in tumor cells activates the anti-tumor immune response. GSEA analysis revealed a group of significantly enriched immune related gene ontologies, such as “Innate immune response”, “Adaptive immune response”, “Response to IFNγ” and “Leukocyte chemotaxis”. Moreover, further network analysis shows that downregulation of FYN enhances the representation of the STAT1 module, a prominent regulator of the immune system [28]. Our data in shFYN tumors, could be explained by IFNγ produced by T cells and NK cells inducing a positive feedback loop in the STAT1 signaling pathway leading to enhanced immune responses and overexpression of IRF-1, IRF8, NLRC5, CIITA. These changes would induce expression of antigen presentation related genes (i.e. TAP1, CXCL9, CCL1, H2-Q4 and H2-DMa, H2-Aa, H2-Ab1) [29,30], as these genes were overexpressed in our RNA-Seq analysis of FYN knockdown glioma models.

Finally, our glioma TME analysis suggests that, at the cellular level, FYN inhibits anti-glioma immunity possibly through the expansion of immune suppressive myeloid cells (MDSCs). We and others have previously reported that glioma infiltrating MDSCs play a key role in inhibiting anti-tumor T-cell immune responses, thus promoting tumor progression [18]. The inhibitory immune-microenvironment in glioma is thought to contribute to the ineffectiveness of immunotherapies [31]. Novel therapeutics approaches that reverse the inhibitory microenvironment are essential to counteract these effects, and we propose that the inhibition of FYN within glioma cells could represent such a strategy.

We propose that inhibition of FYN within glioma cells could be an immune-mediated therapeutic target to restrict MDSC immune suppressive expansion. Since FYN is expressed by both immune cells and tumor cells, therapeutic approaches will need to target FYN specifically in tumor cells. We propose that the combination of tumor cell specific FYN inhibition with other immune-stimulatory treatments, such as immune checkpoint blockade (PDL1-PD1 inhibitors), or Ad-hCMV-TK and Ad-hCMV-Flt3L gene therapy [11,32,33] are promising avenues that are worth of being explored in future experiments.

Funding

Work was supported by National Institutes of Health, NIH/NINDS Grants: R37-NS094804, R01-NS105556 to M.G.C.; NIH/NINDS Grants R01-NS076991, and R01-NS096756 to P.R.L.; NIH/NIBIB: R01-EB022563; NIH/NCI U01CA224160; the Department of Neurosurgery, Rogel Cancer Center at The University of Michigan, ChadTough Foundation, and Leah's Happy Hearts Foundation to M.G.C. and P.R.L. University of Michigan, MICHR Postdoctoral Translational Scholars Program, TL1 TR002240-02, Project F049768 to A.C.

References

1. Reifenberger G, Wirsching HG, Knobbe-Thomsen CB, Weller M. Advances in the molecular genetics of gliomas - implications for classification and therapy. *Nature reviews. Clinical oncology.* 2017; 14(7):434-452.

2. Frattini V, Trifonov V, Chan JM, et al. The integrated landscape of driver genomic alterations in glioblastoma. *Nature genetics.* 2013; 45(10):1141-1149.

3. Lu KV, Zhu S, Cvrljevic A, et al. Fyn and SRC are effectors of oncogenic epidermal growth factor receptor signaling in glioblastoma patients. *Cancer research.* 2009; 69(17):6889-6898.

4. Yadav V, Denning MF. Fyn is induced by Ras/PI3K/Akt signaling and is required for enhanced invasion/migration. *Mol Carcinog.* 2011; 50(5):346-352.

5. Jensen AR, David SY, Liao C, et al. Fyn is downstream of the HGF/MET signaling axis and affects cellular shape and tropism in PC3 cells. *Clinical cancer research : an official journal of the American Association for Cancer Research.* 2011; 17(10):3112-3122.

6. Zhang S, Fan G, Hao Y, Hammell M, Wilkinson JE, Tonks NK. Suppression of protein tyrosine phosphatase N23 predisposes to breast tumorigenesis via activation of FYN kinase. *Genes Dev.* 2017; 31(19):1939-1957.

7. Bowman RL, Wang Q, Carro A, Verhaak RG, Squatrito M. GlioVis data portal for visualization and analysis of brain tumor expression datasets. *Neuro-oncology.* 2017; 19(1):139-141.

8. Lewis-Tuffin LJ, Feathers R, Hari P, et al. Src family kinases differentially influence glioma growth and motility. *Mol Oncol.* 2015; 9(9):1783-1798.

9. Han X, Zhang W, Yang X, et al. The role of Src family kinases in growth and migration of glioma stem cells. *Int J Oncol.* 2014; 45(1):302-310.

10. Preusser M, Lim M, Hafler DA, Reardon DA, Sampson JH. Prospects of immune checkpoint modulators in the treatment of glioblastoma. *Nature reviews. Neurology.* 2015; 11(9):504-514.

11. Ratnam NM, Gilbert MR, Giles AJ. Immunotherapy in CNS cancers: the role of immune cell trafficking. *Neuro-oncology.* 2019; 21(1):37-46.

12. Koschmann C, Calinescu AA, Nunez FJ, et al. ATRX loss promotes tumor growth and impairs nonhomologous end joining DNA repair in glioma. *Sci Transl Med.* 2016; 8(328):328ra328.

13. Núñez FJ, Mendez FM, Kadiyala P, et al. IDH1-R132H acts as a tumor suppressor in glioma via epigenetic up-regulation of the DNA damage response. 2019; 11(479):eaaq1427.

14. Liu KJ, He JH, Su XD, et al. Saracatinib (AZD0530) is a potent modulator of ABCB1-mediated multidrug resistance in vitro and in vivo. *Int J Cancer.* 2013; 132(1):224-235.

15. Yadav VN, Zamler D, Baker GJ, et al. CXCR4 increases in-vivo glioma perivascular invasion, and reduces radiation induced apoptosis: A genetic knockdown study. *Oncotarget.* 2016; 7(50):83701-83719.

16. Calinescu AA, Yadav VN, Carballo E, et al. Survival and Proliferation of Neural Progenitor-Derived Glioblastomas Under Hypoxic Stress is Controlled by a CXCL12/CXCR4 Autocrine-Positive Feedback Mechanism. *Clinical cancer research : an official journal of the American Association for Cancer Research.* 2017; 23(5):1250-1262.

17. Wilson TJ, Zamler DB, Doherty R, Castro MG, Lowenstein PR. Reversibility of glioma stem cells' phenotypes explains their complex in vitro and in vivo behavior: Discovery of a novel neurosphere-specific enzyme, cGMP-dependent protein kinase 1, using the genomic landscape of human glioma stem cells as a discovery tool. *Oncotarget.* 2016; 7(39):63020-63041.

18. Kamran N, Kadiyala P, Saxena M, et al. Immunosuppressive Myeloid Cells' Blockade in the Glioma Microenvironment Enhances the Efficacy of Immune-Stimulatory Gene Therapy. *Molecular therapy : the journal of the American Society of Gene Therapy.* 2017; 25(1):232-248.

19. Elias D, Ditzel HJ. Fyn is an important molecule in cancer pathogenesis and drug resistance. *Pharmacol Res.* 2015; 100:250-254.

20. Saito YD, Jensen AR, Salgia R, Posadas EM. Fyn: a novel molecular target in cancer. *Cancer.* 2010; 116(7):1629-1637.

21. Zheng J, Li H, Xu D, Zhu H. Upregulation of Tyrosine Kinase FYN in Human Thyroid Carcinoma: Role in Modulating Tumor Cell Proliferation, Invasion, and Migration. *Cancer Biother Radiopharm.* 2017; 32(9):320-326.

22. Palacios EH, Weiss A. Function of the Src-family kinases, Lck and Fyn, in T-cell development and activation. *Oncogene.* 2004; 23(48):7990-8000.

23. Yamauchi J, Miyamoto Y, Torii T, et al. Phosphorylation of cytohesin-1 by Fyn is required for initiation of myelination and the extent of myelination during development. *Science signaling.* 2012; 5(243):ra69.

24. Yamaguchi H, Takanashi M, Yoshida N, et al. Saracatinib impairs the peritoneal dissemination of diffuse-type gastric carcinoma cells resistant to Met and fibroblast growth factor receptor inhibitors. *Cancer Sci.* 2014; 105(5):528-536.

25. Lassman AB, Pugh SL, Gilbert MR, et al. Phase 2 trial of dasatinib in target-selected patients with recurrent glioblastoma (RTOG 0627). *Neuro-oncology.* 2015; 17(7):992-998.

26. Jelic D, Mildner B, Kostrun S, et al. Homology modeling of human Fyn kinase structure: discovery of rosmarinic acid as a new Fyn kinase inhibitor and in silico study of its possible binding modes. *Journal of medicinal chemistry.* 2007; 50(6):1090-1100.

27. Zhang S, Qi Q, Chan CB, et al. Fyn-phosphorylated PIKE-A binds and inhibits AMPK signaling, blocking its tumor suppressive activity. *Cell Death Differ.* 2016; 23(1):52-63.

28. Schindler C, Shuai K, Prezioso VR, Darnell JE, Jr. Interferon-dependent tyrosine phosphorylation of a latent cytoplasmic transcription factor. *Science (New York, N.Y.).* 1992; 257(5071):809-813.

29. Majoros A, Platanitis E, Kernbauer-Holzl E, Rosebrock F, Muller M, Decker T. Canonical and Non-Canonical Aspects of JAK-STAT Signaling: Lessons from Interferons for Cytokine Responses. *Frontiers in immunology.* 2017; 8:29.

30. Avalle L, Pensa S, Regis G, Novelli F, Poli V. STAT1 and STAT3 in tumorigenesis: A matter of balance. *Jak-stat.* 2012; 1(2):65-72.

31. Kamran N, Chandran M, Lowenstein PR, Castro MG. Immature myeloid cells in the tumor microenvironment: Implications for immunotherapy. *Clinical immunology (Orlando, Fla.).* 2018; 189:34-42.

32. Ivashkiv LB. IFNgamma: signalling, epigenetics and roles in immunity, metabolism, disease and cancer immunotherapy. *Nature reviews. Immunology.* 2018; 18(9):545-558.

33. Kamran N, Alghamri MS, Nunez FJ, et al. Current state and future prospects of immunotherapy for glioma. *Immunotherapy.* 2018; 10(4):317-339.

Figure 1. FYN is a potential regulator of aggressiveness in mouse and human glioma. (A) FYN tyrosine signals downstream from mutated RTK driver genes. Red: mutation/amplification, green: mutation/deletion, orange: overexpression. **(B)** FYN levels correlate positively with glioma cell malignancy in WB analysis comparing FYN, SRC, P-SFK-Tyrosine-416 and P-SFK-Tyrosine-530 levels in mouse (GL26, NP, NPA, NPAI) and human (MGG8-Sphere and MGG8-Adherent) glioma cells; loading control = β-actin. **(C)** Network of DE genes in malignant NPA vs less malignant NPAI mouse glioma stem cells. FYN is the largest yellow octagon. Cluster of nodes of identical color represents a module of highly interacting genes. The FYN network is highlighted in yellow. (**D)** Right panel: the FYN network; FYN has a degree of 63. **(E)** Network analysis of DE genes of increased malignant MGG8-Spheres, vs less malignant MGG8-Adherent human glioma stem cells; FYN is the large octagon. **(F)** FYN's network in human cells. Red lines indicate edges connecting nodes to FYN; FYN's degree is 47.

Figure 2. Knocking down FYN in GEMM prolongs animal survival. (A-C) Kaplan–Meier survival curves of SB mouse glioma models demonstrate that animals bearing FYN knockdown tumors have increased median survival (MS). **(A)** NP (MS: 94 days; n: 15) versus NPF (MS: 131 days; n: 29). (**B)** NPA (MS: 80 days; n: 16) versus NPAF (MS: 142 days; n: 28). **(C)** NPD (MS: 69 days; n: 15) versus NPDF (MS: 108 days; n: 23). Log-rank (Mantel-Cox) test; *** $p<0.001$, ****$p<0.0001$. **(D-F, top)** FYN expression in tumors (green = tumor; and Blue = DAPI stained nuclei), quantified as fluorescence integrated density using Image-J **(D-F, bottom)**; n=5 per condition, scale bar = 50 μm. Ten random fields per tumor section per animal were imaged. Bars ±SEM are shown; (***$p<0.001$, *$p<0.05$ using linear mixed effect models) (**G-I).** Histopathological analysis was performed in tumor sections stained with H&E; shFYN tumors were compared with controls. Scale bars: 100 μm. P: pseudo-palisades, N: necrosis, H: hemorrhage, VP: vascular proliferation, MS: mesenchymal component, SC: small cells, G: giant cells. **(J)** Table representing

histopathological semi-quantitative analysis: very low (+/-), low (+), medium (++) and high (+++). **(K-M)** Cell proliferation analysis: Positive P-H3-S10 cells were counted by Image-J software. Scale bars: 50 µm. P-H3-S10 positive cells per total cells in the visual field; n=5. Ten fields of each section were selected at random. Error bars represent ±SEM; linear mixed effect models, ***p<0.001, **p<0.01.

Figure 3. Enrichment in immune-related pathways as potential mechanisms involved in FYN-mediated tumor growth control. (A) Volcano plot displays the DE genes from SB NPF vs NP mouse GEMM. DE genes (n=567) were selected based on the fold change (≥ 1.5) and a q-value (FDR corrected p-value) of < 0.05. Upregulated genes (n=226; red dots) and downregulated genes (n=341; green dots) are shown. Example of genes upregulated (blue triangles) or downregulated (yellow triangles) are indicated in the lower right quadrant. Two-sided Student's t-test was performed to determine statistical significance. **(B)** Network analysis of the DE genes comparing NPF vs NP mouse gliomas. Large octagonal nodes represent networks hubs. Clusters of the same color represents modules of highly interacting genes. Red border: upregulated genes. Green borders: downregulated genes. **(C)** Functional enrichment analysis of pathways for each module. The bar graph shows the overrepresented pathways plotted according to the -log2 FDR q-value (FDR). Cutoff of q-value ≤0.01.

Figure 4. FYN downregulation increases immune response related gene ontologies

(A) Gene set enrichment analysis (GSEA) of DE genes comparing NPF tumors versus NP tumors. Enrichment map of the most significantly upregulated GO terms (red nodes) in NPF gliomas at FDR<0.1 and p<0.05. Node color indicates p-value; size indicates the frequency of the GO term in the GO database. **(B)** Functional enrichment analysis of upregulated GO terms in NPF tumors compared with NP. Cutoff at (NES) >1.87 and q-value<0.1. Enrichment plots of two of the most significant GO terms: "Immune response" (top panel) and "Cell Chemotaxis" (lower panel) are

shown. These plots indicate the profile of the Running ES Score & Positions of GeneSet Members. **(C)** Heat maps illustrate gene expression pattern for Immune Response (left panel) and Cell Chemotaxis (right panel) GO terms in NPF vs. NP tumors. Upregulated genes are represented in red and downregulated genes are represented in green (q-value ≤ 0.05 and fold change ≥ ± 1.5). Brackets highlight DE genes present in upregulated immune GOs: “Innate Immune Response”, “Adaptive Immune Response”, “Response to Interferon Gamma” and “leukocyte chemotaxis”.

Figure 5. Tumor growth delay and increased survival in FYN downregulated gliomas is immune mediated.

(A-B) Kaplan–Meier survival curves for glioma in C57BL/6 immune-competent mice. **(A)** NP-FYN knockdown gliomas displayed significant increases in MS: 27 vs 34 days; *p=0.011. **(B)** Mice bearing gliomas with NPA-FYN knockdown displayed significant increase in MS: 20 vs 30 days; **p=0.0031 compared to the control; n=5. FYN expression was detected by immunofluorescence. Tumor: green; Nuclei: blue; scale bars: 50 μm. **(C-D)** Kaplan–Meier survival curves in NSG immune-compromised mice. **(C)** NP-FYN knockdown gliomas displayed no significant increases in MS (24 vs 26 days; p=0.06) n=9/10. **(D)** NPA-FYN knockdown displayed a minor increase in MS (22 vs 24 days; *p=0.044); n=5. **(E)** Kaplan–Meier survival curve for NP-NT vs NP-shFYN glioma in CD8 KO immune-deficient mice. No significant difference was observed in survival. **(F)** Kaplan–Meier survival curve for NPA-NT vs NPA-shFYN glioma in CD8 KO immune-deficient mice. No significant difference was observed in survival; n=5. Statistics were assessed using the log-rank Mantel-Cox test.

Figure 6. Downregulation of FYN in glioma modulates immune responses through MDSC reduction. Immune cells within the TME of NPA-NT or NPA-shFYN tumors were analyzed by flow cytometry. **(A-B)** Percentage of CD4-T ($CD4^+$, $CD3^+$) cells within the $CD45^+$ cell population.

Representative flow plots for each group are displayed. ns= non-significant; unpaired t-test. Graph represent mean ± SEM (n= 10). **(C-D)** Percentage of CD8-T cells ($CD8^+$, $CD3^+$) within the $CD45^+$ cell population. Representative flow plots for each group are displayed. Graph represents mean ± SEM (n= 10); ns= non-significant; unpaired t-test. **(E)** Percentage of monocytic myeloid derived suppressor cells (M-MDSCs: CD11b+, Ly6Chi, Ly6G-) within the $CD45^+$ cell population. Bars represent mean ± SEM (n= 10); *p<0.05; unpaired t-test. **(F)** Percentage of polymorphonuclear myeloid derived suppressor cells (PMN-MDSCs: CD45+, CD11b+, Ly6Clo, Ly6G+) within the $CD45^+$ cell population Graph represent mean ± SEM (n= 10); *p<0.05; unpaired t-test. **(G)** Representative flow plots of M-MDSC and PMN-MDSC cell analysis. **(H-I)** Percentage of macrophages within the $CD45^+$ cell population. Graph shows mean ± SEM (n= 10); ns= non-significant; unpaired t-test. **(J-K)** Geometric mean of MHC II^+ expression in macrophages within the $CD45^+$ cell population. Representative flow plots for each group. Graph represent mean ± SEM; n= 10; ns= non-significant; unpaired t-test.

Figure 1

A

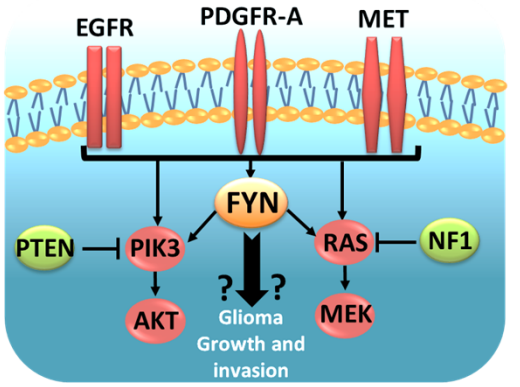

B

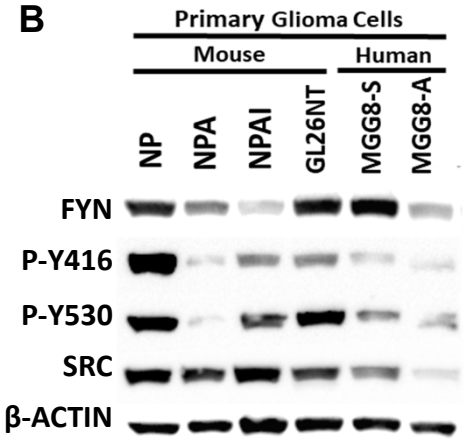

C

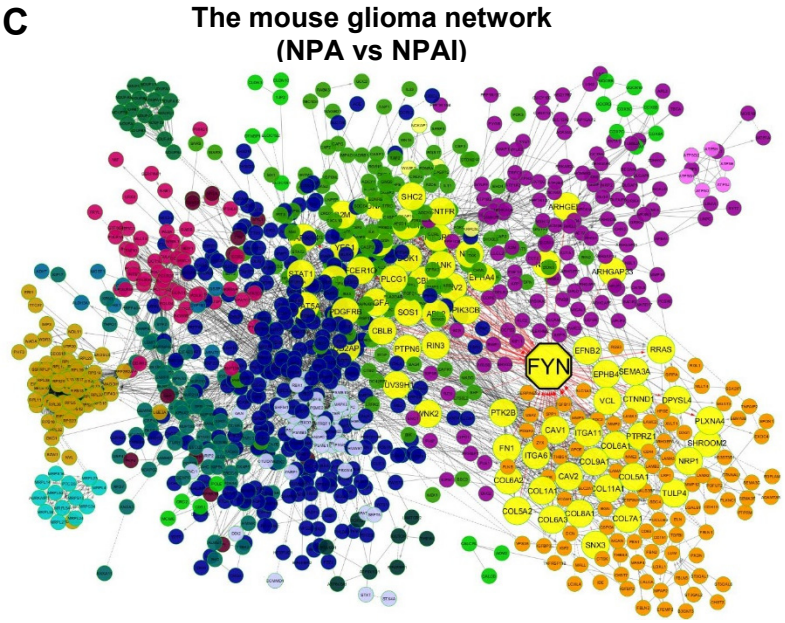

D

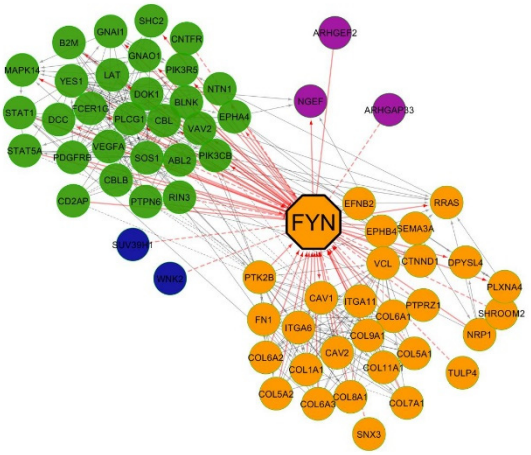

E

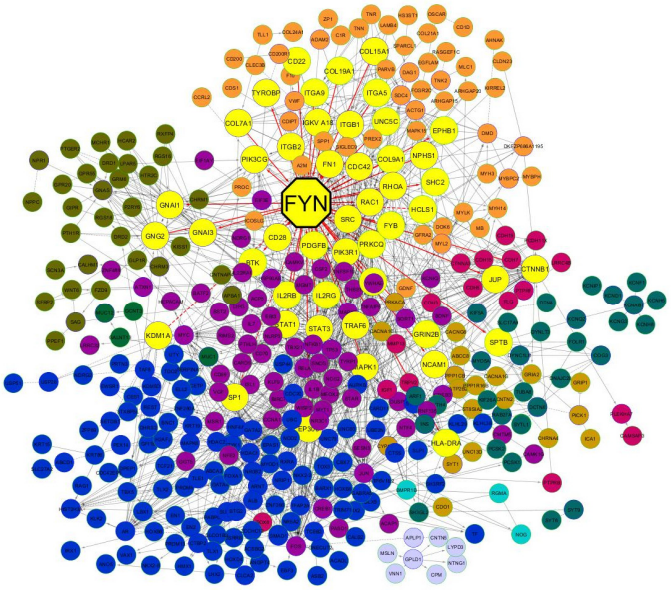

F

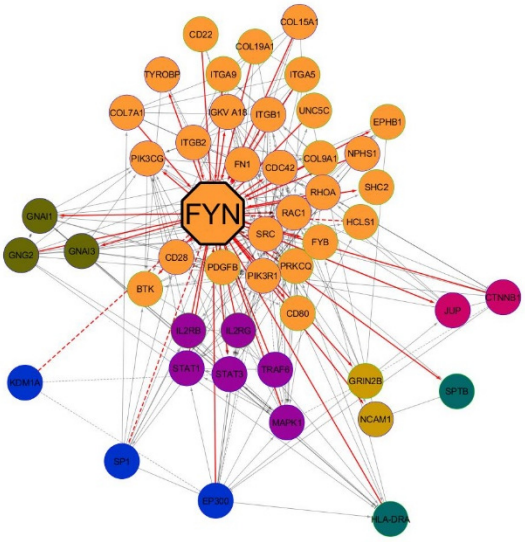

Figure 2

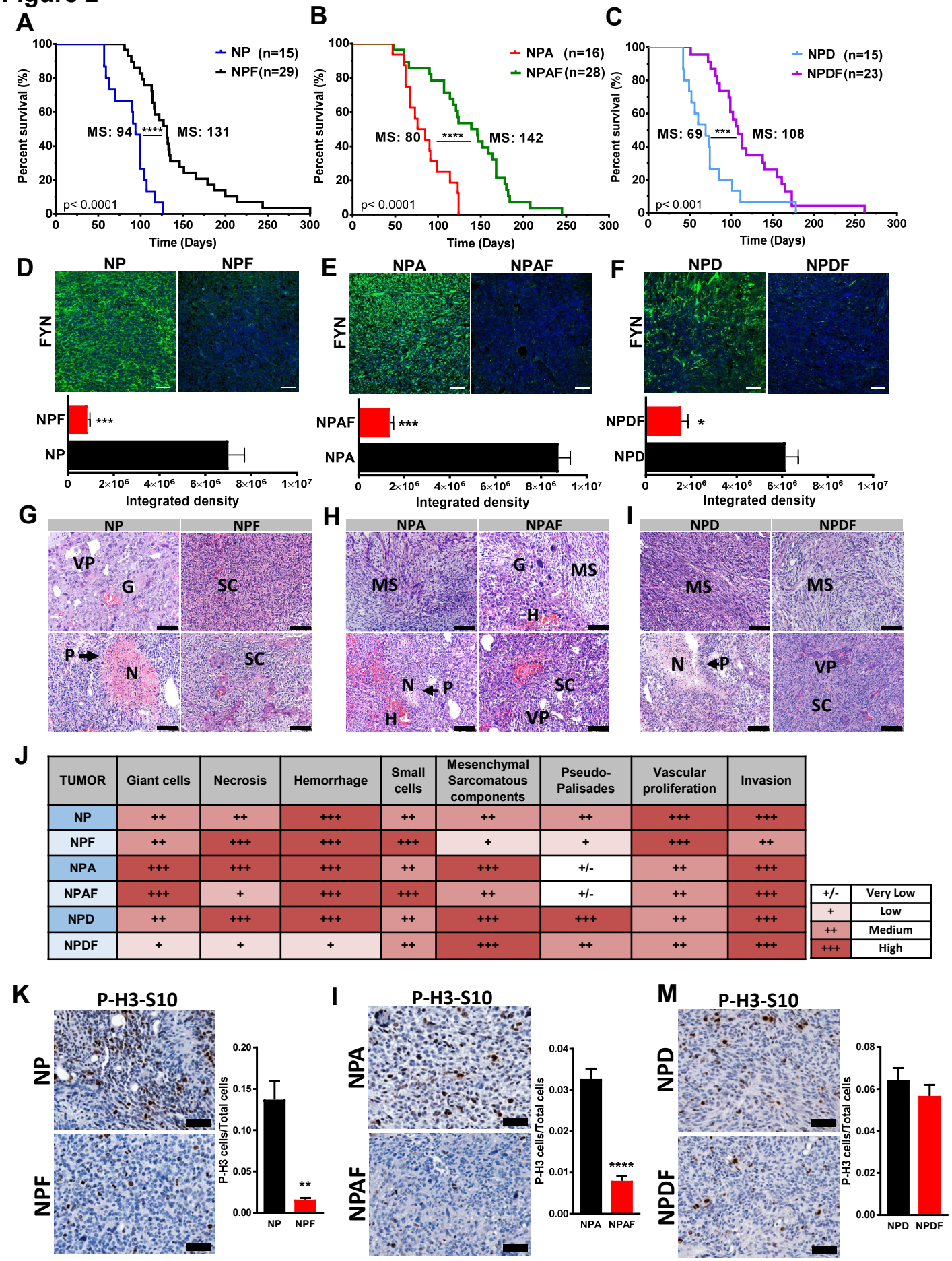

TUMOR	Giant cells	Necrosis	Hemorrhage	Small cells	Mesenchymal Sarcomatous components	Pseudo-Palisades	Vascular proliferation	Invasion
NP	++	++	+++	++	++	++	+++	+++
NPF	++	+++	+++	+++	+	+	+++	++
NPA	+++	+++	+++	++	+++	+/-	++	+++
NPAF	+++	+	+++	+++	++	+/-	++	+++
NPD	++	+++	+++	++	+++	+++	++	+++
NPDF	+	+	+	++	+++	++	++	+++

+/-	Very Low
+	Low
++	Medium
+++	High

Figure 3

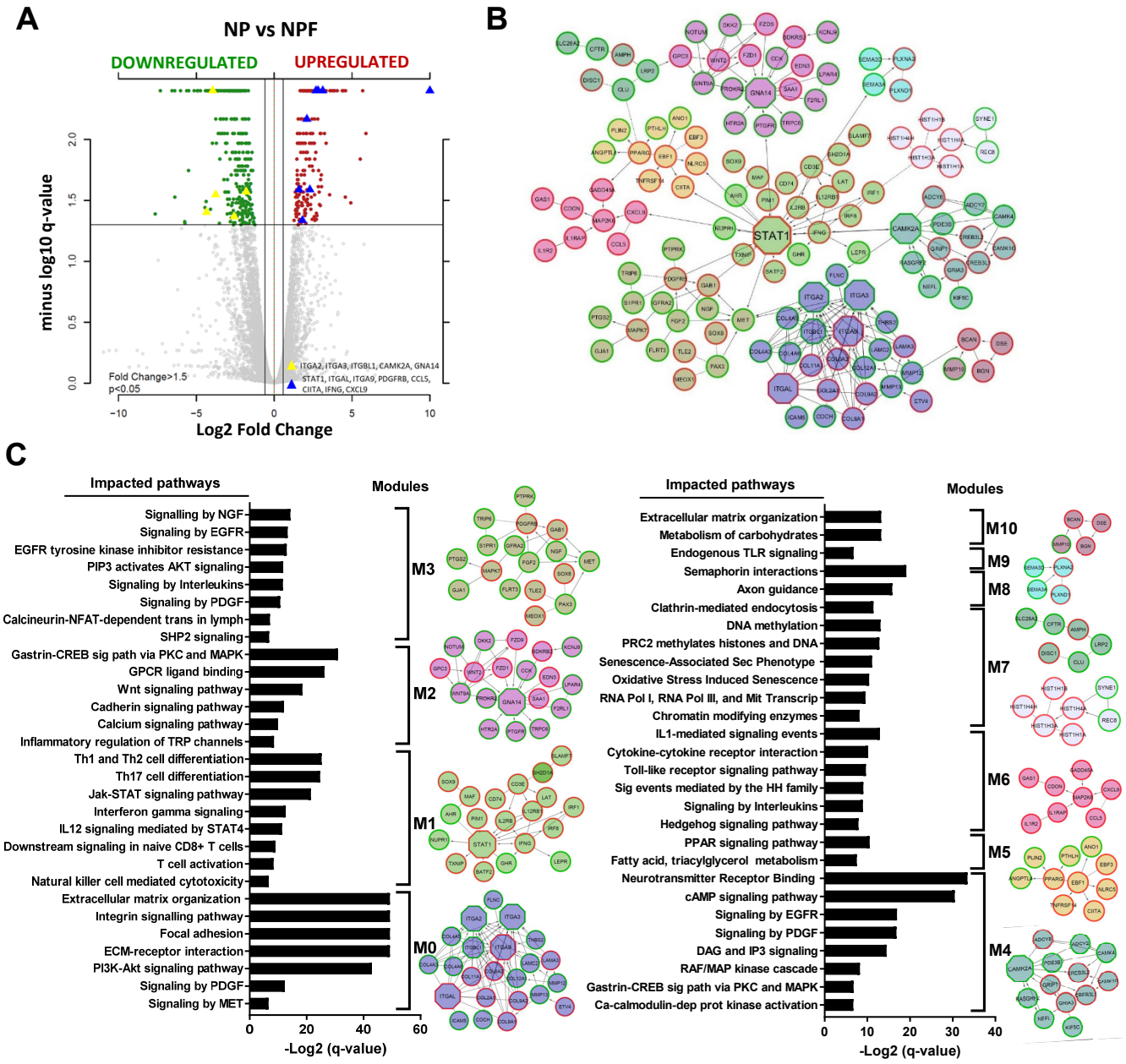
A
NP vs NPF
DOWNREGULATED
UPREGULATED
minus log10 q-value
Log2 Fold Change
Fold Change>1.5
p<0.05
ITGA2, ITGA3, ITGBL1, CAMK2A, GNA14
STAT1, ITGAL, ITGA9, PDGFRB, CCL5,
CIITA, IFNG, CXCL9
B
STAT1
C
Impacted pathways
Modules
Signalling by NGF
Signaling by EGFR
EGFR tyrosine kinase inhibitor resistance
PIP3 activates AKT signaling
Signaling by Interleukins
Signaling by PDGF
Calcineurin-NFAT-dependent trans in lymph
SHP2 signaling
Gastrin-CREB sig path via PKC and MAPK
GPCR ligand binding
Wnt signaling pathway
Cadherin signaling pathway
Calcium signaling pathway
Inflammatory regulation of TRP channels
Th1 and Th2 cell differentiation
Th17 cell differentiation
Jak-STAT signaling pathway
Interferon gamma signaling
IL12 signaling mediated by STAT4
Downstream signaling in naive CD8+ T cells
T cell activation
Natural killer cell mediated cytotoxicity
Extracellular matrix organization
Integrin signalling pathway
Focal adhesion
ECM-receptor interaction
PI3K-Akt signaling pathway
Signaling by PDGF
Signaling by MET
M3
M2
M1
M0
-Log2 (q-value)
Impacted pathways
Modules
Extracellular matrix organization
Metabolism of carbohydrates
Endogenous TLR signaling
Semaphorin interactions
Axon guidance
Clathrin-mediated endocytosis
DNA methylation
PRC2 methylates histones and DNA
Senescence-Associated Sec Phenotype
Oxidative Stress Induced Senescence
RNA Pol I, RNA Pol III, and Mit Transcrip
Chromatin modifying enzymes
IL1-mediated signaling events
Cytokine-cytokine receptor interaction
Toll-like receptor signaling pathway
Sig events mediated by the HH family
Signaling by Interleukins
Hedgehog signaling pathway
PPAR signaling pathway
Fatty acid, triacylglycerol metabolism
Neurotransmitter Receptor Binding
cAMP signaling pathway
Signaling by EGFR
Signaling by PDGF
DAG and IP3 signaling
RAF/MAP kinase cascade
Gastrin-CREB sig path via PKC and MAPK
Ca-calmodulin-dep prot kinase activation
M10
M9
M8
M7
M6
M5
M4
-Log2 (q-value)

Figure 4

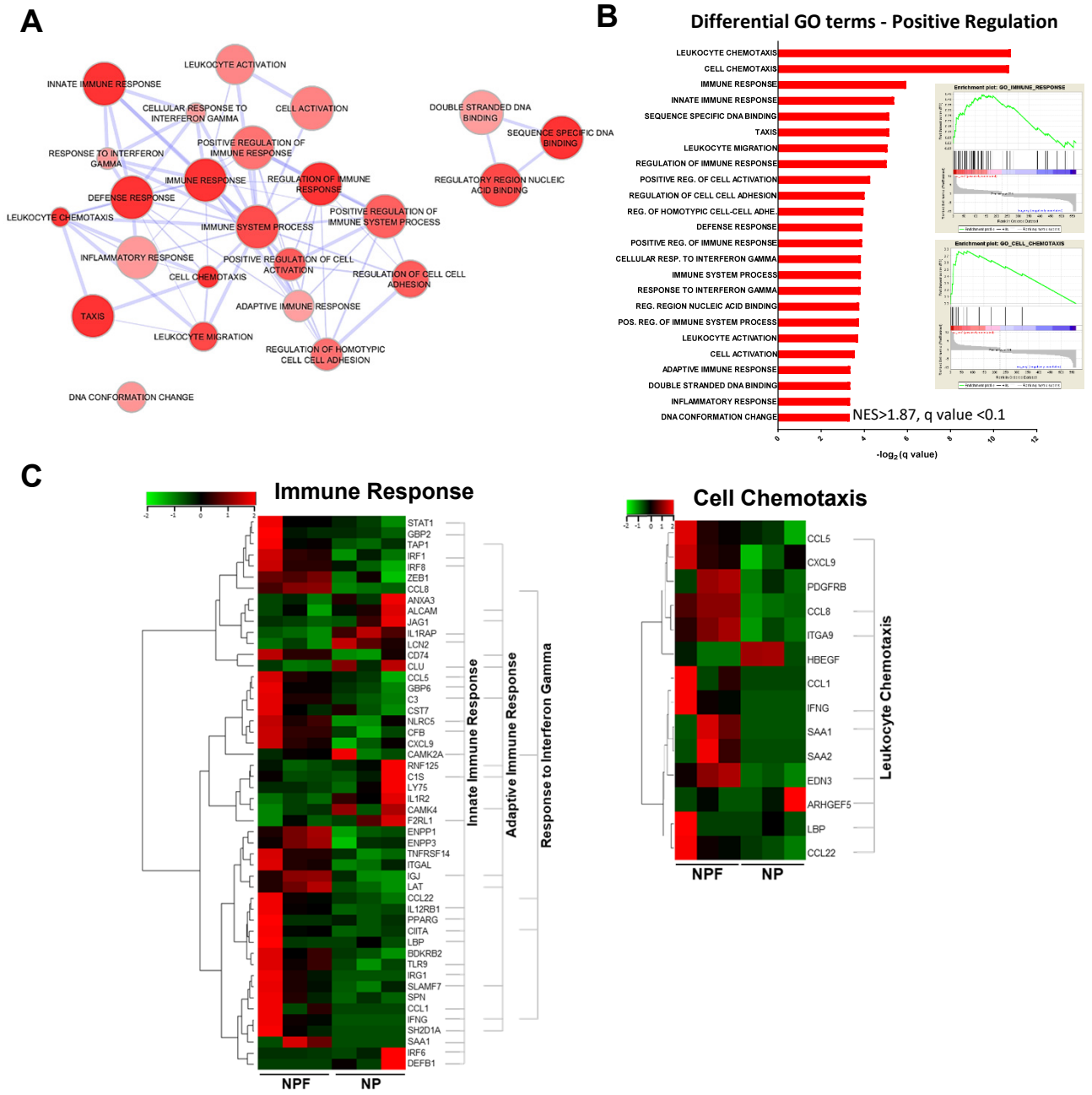
A
LEUKOCYTE ACTIVATION
INNATE IMMUNE RESPONSE
CELLULAR RESPONSE TO INTERFERON GAMMA
CELL ACTIVATION
DOUBLE STRANDED DNA BINDING
SEQUENCE SPECIFIC DNA BINDING
POSITIVE REGULATION OF IMMUNE RESPONSE
RESPONSE TO INTERFERON GAMMA
IMMUNE RESPONSE
REGULATION OF IMMUNE RESPONSE
REGULATORY REGION NUCLEIC ACID BINDING
DEFENSE RESPONSE
LEUKOCYTE CHEMOTAXIS
IMMUNE SYSTEM PROCESS
POSITIVE REGULATION OF IMMUNE SYSTEM PROCESS
INFLAMMATORY RESPONSE
POSITIVE REGULATION OF CELL ACTIVATION
CELL CHEMOTAXIS
REGULATION OF CELL CELL ADHESION
ADAPTIVE IMMUNE RESPONSE
TAXIS
LEUKOCYTE MIGRATION
REGULATION OF HOMOTYPIC CELL CELL ADHESION
DNA CONFORMATION CHANGE
B
Differential GO terms - Positive Regulation
LEUKOCYTE CHEMOTAXIS
CELL CHEMOTAXIS
IMMUNE RESPONSE
INNATE IMMUNE RESPONSE
SEQUENCE SPECIFIC DNA BINDING
TAXIS
LEUKOCYTE MIGRATION
REGULATION OF IMMUNE RESPONSE
POSITIVE REG. OF CELL ACTIVATION
REGULATION OF CELL CELL ADHESION
REG. OF HOMOTYPIC CELL-CELL ADHE.
DEFENSE RESPONSE
POSITIVE REG. OF IMMUNE RESPONSE
CELLULAR RESP. TO INTERFERON GAMMA
IMMUNE SYSTEM PROCESS
RESPONSE TO INTERFERON GAMMA
REG. REGION NUCLEIC ACID BINDING
POS. REG. OF IMMUNE SYSTEM PROCESS
LEUKOCYTE ACTIVATION
CELL ACTIVATION
ADAPTIVE IMMUNE RESPONSE
DOUBLE STRANDED DNA BINDING
INFLAMMATORY RESPONSE
DNA CONFORMATION CHANGE
NES>1.87, q value <0.1
-log2 (q value)
C
Immune Response
STAT1
GBP2
TAP1
IRF1
IRF8
ZEB1
CCL8
ANXA3
ALCAM
JAG1
IL1RAP
LCN2
CD74
CLU
CCL5
GBP6
C3
CST7
NLRC5
CFB
CXCL9
CAMK2A
RNF125
C1S
LY75
IL1R2
CAMK4
F2RL1
ENPP1
ENPP3
TNFRSF14
ITGAL
IGJ
LAT
CCL22
IL12RB1
PPARG
CIITA
LBP
BDKRB2
TLR9
IRG1
SLAMF7
SPN
CCL1
IFNG
SH2D1A
SAA1
IRF6
DEFB1
Innate Immune Response
Adaptive Immune Response
Response to Interferon Gamma
NPF
NP
Cell Chemotaxis
CCL5
CXCL9
PDGFRB
CCL8
ITGA9
HBEGF
CCL1
IFNG
SAA1
SAA2
EDN3
ARHGEF5
LBP
CCL22
Leukocyte Chemotaxis
NPF
NP

Figure 5

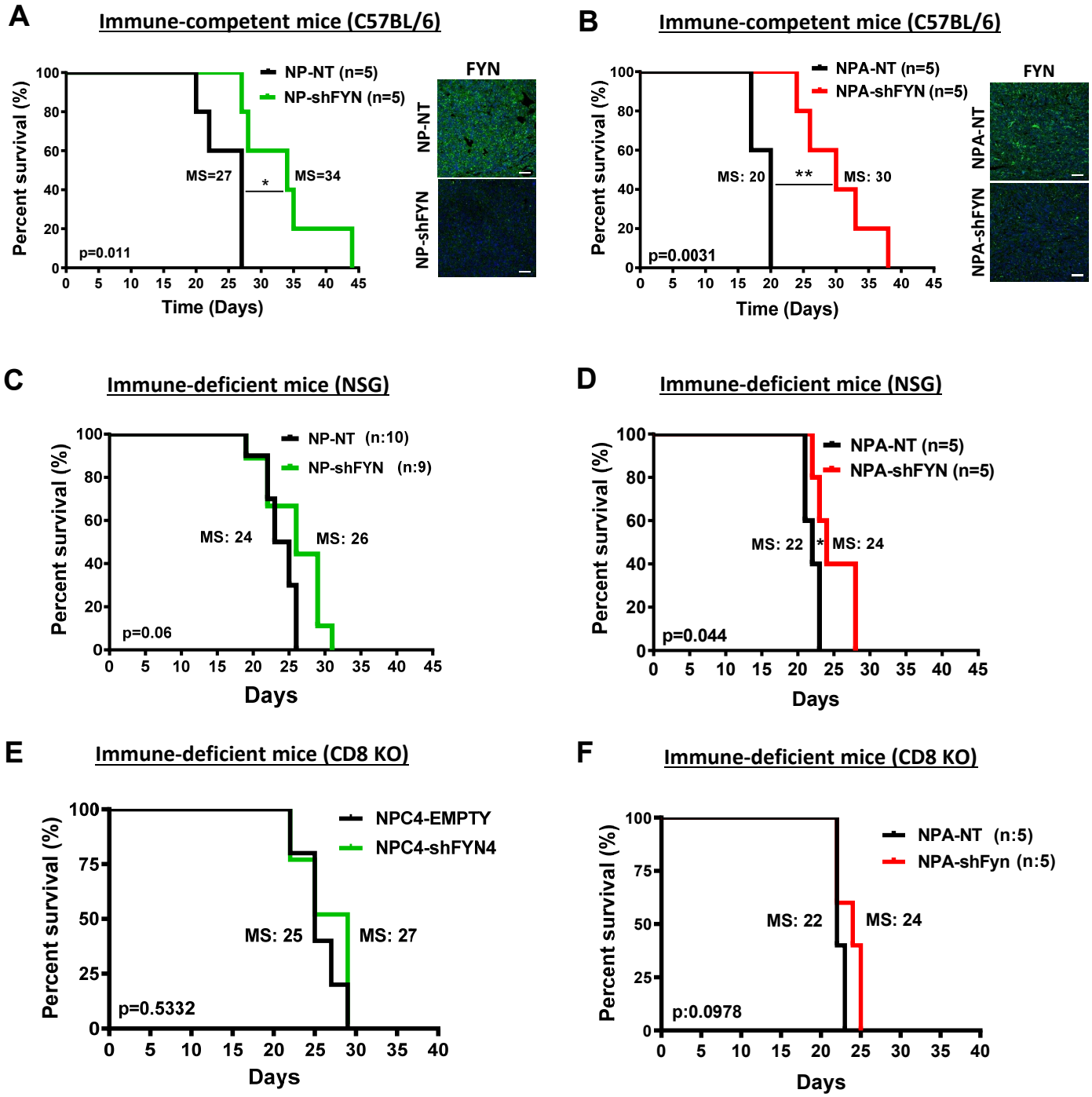
A
Immune-competent mice (C57BL/6)
NP-NT (n=5)
NP-shFYN (n=5)
Percent survival (%)
Time (Days)
MS=27
MS=34
*
p=0.011
FYN
NP-NT
NP-shFYN
B
Immune-competent mice (C57BL/6)
NPA-NT (n=5)
NPA-shFYN (n=5)
Percent survival (%)
Time (Days)
MS: 20
MS: 30
**
p=0.0031
FYN
NPA-NT
NPA-shFYN
C
Immune-deficient mice (NSG)
NP-NT (n:10)
NP-shFYN (n:9)
Percent survival (%)
Days
MS: 24
MS: 26
p=0.06
D
Immune-deficient mice (NSG)
NPA-NT (n=5)
NPA-shFYN (n=5)
Percent survival (%)
Days
MS: 22
*
MS: 24
p=0.044
E
Immune-deficient mice (CD8 KO)
NPC4-EMPTY
NPC4-shFYN4
Percent survival (%)
Days
MS: 25
MS: 27
p=0.5332
F
Immune-deficient mice (CD8 KO)
NPA-NT (n:5)
NPA-shFyn (n:5)
Percent survival (%)
Days
MS: 22
MS: 24
p:0.0978

Figure 6

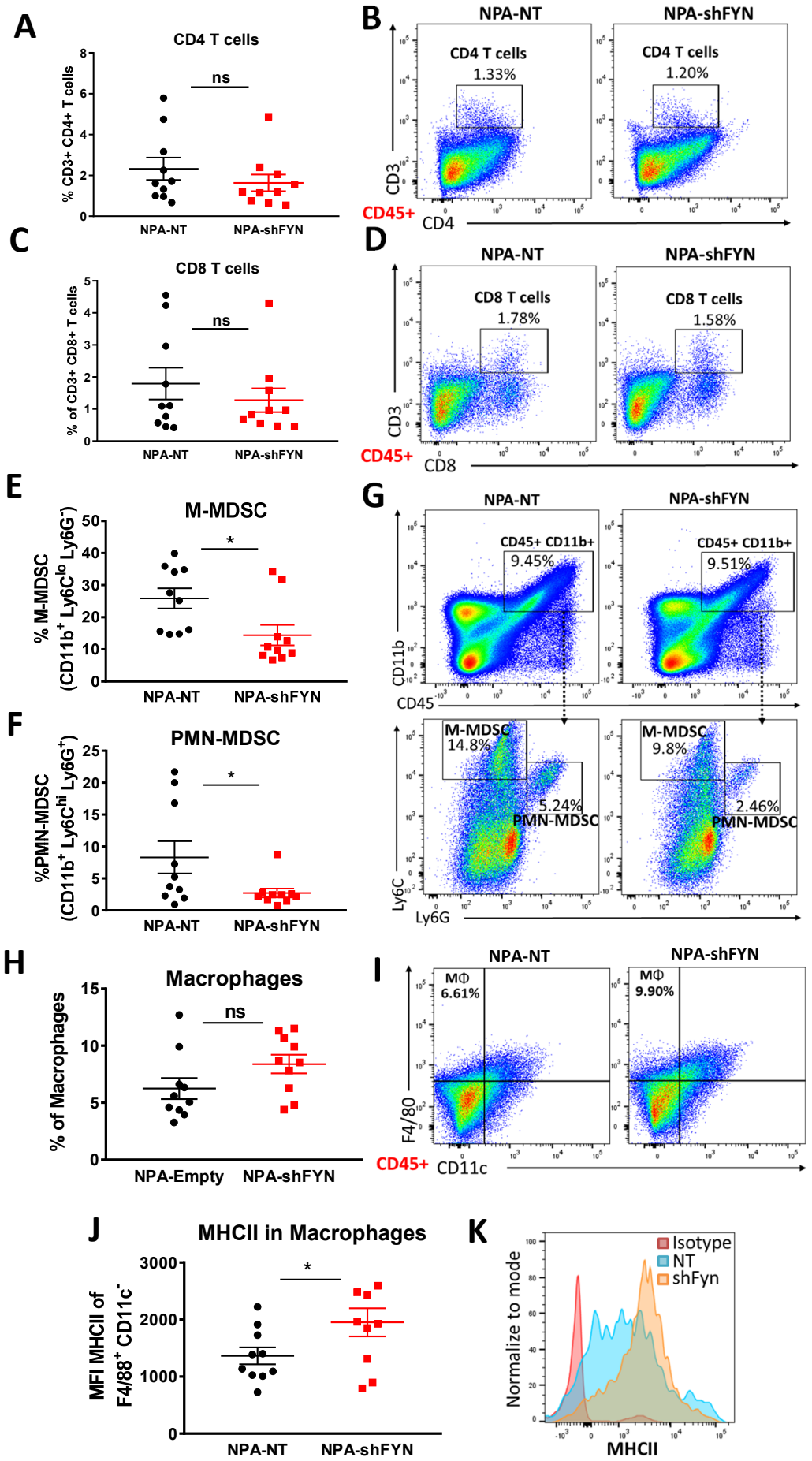
A
CD4 T cells
% CD3+ CD4+ T cells
ns
NPA-NT
NPA-shFYN
B
NPA-NT
NPA-shFYN
CD4 T cells
1.33%
CD4 T cells
1.20%
CD3
CD45+
CD4
C
CD8 T cells
% of CD3+ CD8+ T cells
ns
NPA-NT
NPA-shFYN
D
NPA-NT
NPA-shFYN
CD8 T cells
1.78%
CD8 T cells
1.58%
CD3
CD45+
CD8
E
M-MDSC
% M-MDSC
(CD11b+ Ly6Clo Ly6G-)
*
NPA-NT
NPA-shFYN
F
PMN-MDSC
%PMN-MDSC
(CD11b+ Ly6Chi Ly6G+)
*
NPA-NT
NPA-shFYN
G
NPA-NT
NPA-shFYN
CD45+ CD11b+
9.45%
CD45+ CD11b+
9.51%
CD11b
CD45
M-MDSC
14.8%
5.24%
PMN-MDSC
M-MDSC
9.8%
2.46%
PMN-MDSC
Ly6C
Ly6G
H
Macrophages
% of Macrophages
ns
NPA-Empty
NPA-shFYN
I
NPA-NT
NPA-shFYN
MΦ
6.61%
MΦ
9.90%
F4/80
CD45+
CD11c
J
MHCII in Macrophages
MFI MHCII of
F4/88+ CD11c-
*
NPA-NT
NPA-shFYN
K
Isotype
NT
shFyn
Normalize to mode
MHCII